ARL-TR-10329 ● APR 2026

TiltRotor Aeroelastic Stability Testbed (TRAST) Rotor Hub Analysis and Testing Results

Benjamin Cobb and Andrew R. Kreshock

NOTICES

Disclaimers

ARL-TR-10329 ● APR 2026

TiltRotor Aeroelastic Stability Testbed (TRAST) Rotor Hub Analysis and Testing

Benjamin Cobb
SURVICE Engineering

Andrew R. Kreshock
DEVCOM Army Research Laboratory

REPORT DOCUMENTATION PAGE

1. REPORT DATE	2. REPORT TYPE	3. DATES COVERED START DATE	3. DATES COVERED END DATE
April 2026	Technical Report	October 2024	January 2025

4. TITLE AND SUBTITLE
TiltRotor Aeroelastic Stability Testbed (TRAST) Rotor Hub Analysis and Testing Results

5a. CONTRACT NUMBER	5b. GRANT NUMBER	5c. PROGRAM ELEMENT NUMBER
5d. PROJECT NUMBER	**5e. TASK NUMBER**	**5f. WORK UNIT NUMBER**

6. AUTHOR(S)
Benjamin Cobb and Andrew R. Kreshock

7. PERFORMING ORGANIZATION NAME(S) AND ADDRESS(ES)
DEVCOM Army Research Laboratory
ATTN: FCDD-RLA-WF
Aberdeen Proving Ground, MD 21005

8. PERFORMING ORGANIZATION REPORT NUMBER
ARL-TR-10329

9. SPONSORING/MONITORING AGENCY NAME(S) AND ADDRESS(ES)	10. SPONSOR/MONITOR'S ACRONYM(S)	11. SPONSOR/MONITOR'S REPORT NUMBER(S)

12. DISTRIBUTION/AVAILABILITY STATEMENT
DISTRIBUTION STATEMENT A. Approved for public release: distribution unlimited.

13. SUPPLEMENTARY NOTES
ORCIDs: Benjamin Cobb, 0009-0006-0214-8000; Andrew R. Kreshock, 0009-0001-0693-1645

14. ABSTRACT
The TiltRotor Aeroelastic Stability Testbed (TRAST) is a semi-span aeroelastic tiltrotor testbed, developed by the U.S. Army and NASA, used to investigate whirl-flutter stability of tiltrotor aircraft. Understanding the modal behavior of the rotor is an important step in successfully modeling the testbed as a whole. The TRAST model has two primary hub configurations: gimballed and hingeless. Ground vibration testing was conducted to provide baseline frequencies and trends for the four primary rotor modes (symmetric and asymmetric flap and lag) and to compare them with analytical data from RCAS, NASTRAN, and CAMRAD II (hingeless hub only) models to validate the models and demonstrate their efficacy in predicting the vibratory modes of the hub. Both configurations of the hub were experimentally excited using an impact hammer with blade pitch angles ranging from –5° to 65°. The frequency responses were measured using a series of accelerometers, allowing the frequency of each mode to be determined. The results of the test demonstrate reasonable agreement between analytical and experimental results for both the hingeless and gimballed. Additionally, the hingeless hub's frequency response is demonstrated to follow the same general trends as the gimballed hub throughout the collective range, albeit with the large increase in frequency one would expect from the stiffer configuration.

15. SUBJECT TERMS
TiltRotor, Ground Vibration Testing, GVT, Aeroelasticity, Rotorcraft Comprehensive Analysis System, RCAS, Comprehensive Analytical Model of Rotorcraft Aerodynamics and Dynamics, CAMRAD, Rotorcraft, Weapons Sciences

16. SECURITY CLASSIFICATION OF: a. REPORT	b. ABSTRACT	C. THIS PAGE	17. LIMITATION OF ABSTRACT	18. NUMBER OF PAGES
UNCLASSIFIED	UNCLASSIFIED	UNCLASSIFIED	UU	24

19a. NAME OF RESPONSIBLE PERSON	19b. PHONE NUMBER *(Include area code)*
Benjamin Cobb	(520) 851-0609

STANDARD FORM 298 (REV. 5/2020)
Prescribed by ANSI Std. Z39.18

Contents

List of Figures

List of Tables

1. Introduction

The TiltRotor Aeroelastic Stability Testbed (TRAST) is a multiconfiguration testbed for wind tunnel and hovercell testing. The testbed is designed to investigate whirl-flutter stability and other aeroelastic phenomena associated with tiltrotor aircraft. The model consists of a dynamically scaled right-hand wing, a rigid fuselage/fairing, and a pylon that supports a dynamically scaled 8-ft-diameter rotor, which is operated in windmilling mode for stability testing (Figure 1). This model has two primary hub configurations: gimballed and hingeless. The gimballed hub design prevents the transfer of rotor out-of-plane bending moments through the shaft while the hingeless hub cantilevers the blade spindles and allows these moments to transfer from the rotating frame into the rest of the model. The model also has two blade sets: one carbon fiber and one fiberglass. The blades were manufactured using the same construction methodology and molds, with the only major difference being the composite used for the layups. As is typical, the fiberglass composite produced more flexible blades while the carbon fiber blades are significantly stiffer and stronger.

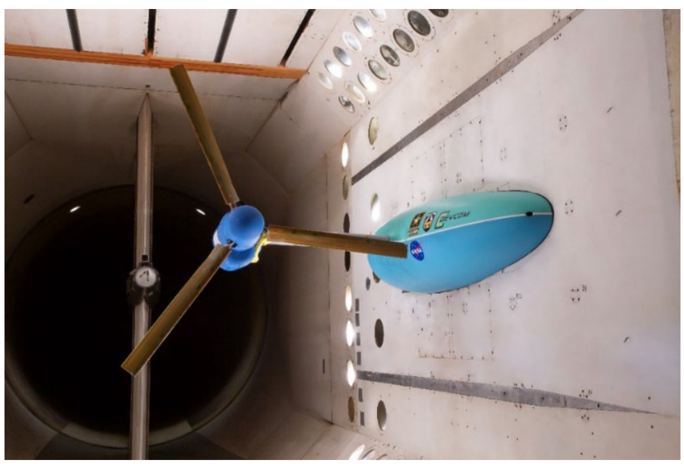

Figure 1. TRAST installed in the transonic dynamics tunnel.

Understanding the behavior of the different hub configurations in an isolated setting is an important precursor to investigating their potential impacts on tiltrotor stability and vibratory response in preparation for wind tunnel testing. Rotorcraft analysis software provide excellent tools for analytical modeling, but the fidelity of these models and their agreement with experimental results must be understood and characterized before relying on them. To evaluate the accuracy of the analytical models developed in Rotorcraft Comprehensive Analysis System (RCAS) and Comprehensive Analytical Model of Rotorcraft Aerodynamics and Dynamics (CAMRAD II) for both rotor hubs, a comparative study was performed using experimental data collected from ground vibration testing (GVT).

2. Ground Vibration Testing

GVT was conducted on both the hingeless and gimballed rotor hubs in a simulated free-free environment to allow for the extraction of useful modal frequency data. Each hub in turn was mounted on a 3-D printed shaft that has a slotted baseplate installed (Figure 2). Nylon all-thread rods were then connected to the pitch horns on each rotor hub, with the bottom end secured to the slotted baseplate, allowing for blade pitch angle adjustment. The hubs were then suspended from a single spring such that the suspension line was approximately coaxial with the central shaft (Figure 3). The blades were then installed on each hub—fiberglass on the gimballed hub and carbon fiber on the hingeless hub—to reflect the primary setups used, or intended for use, on their respective hubs during wind tunnel and hovercell testing.

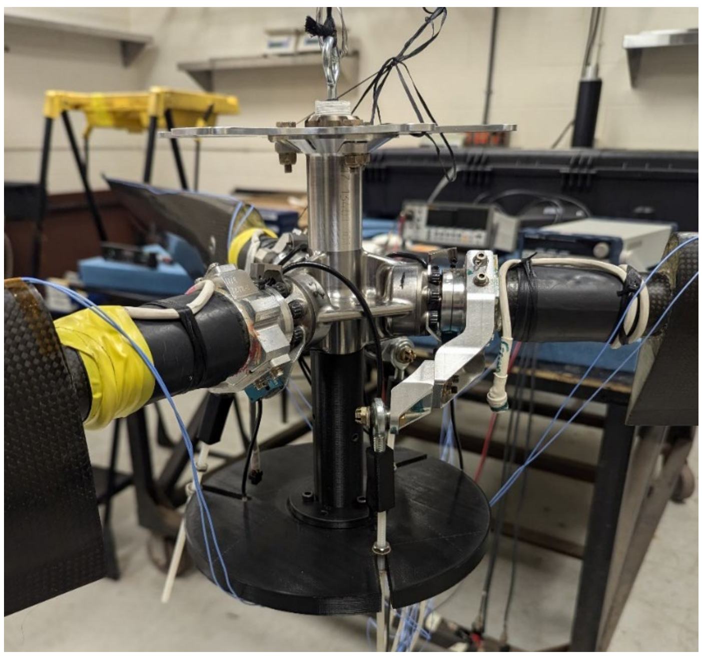

Figure 2. Hingeless hub (with carbon fiber blades) installed on 3-D printed baseplate with nylon pitch control rods.

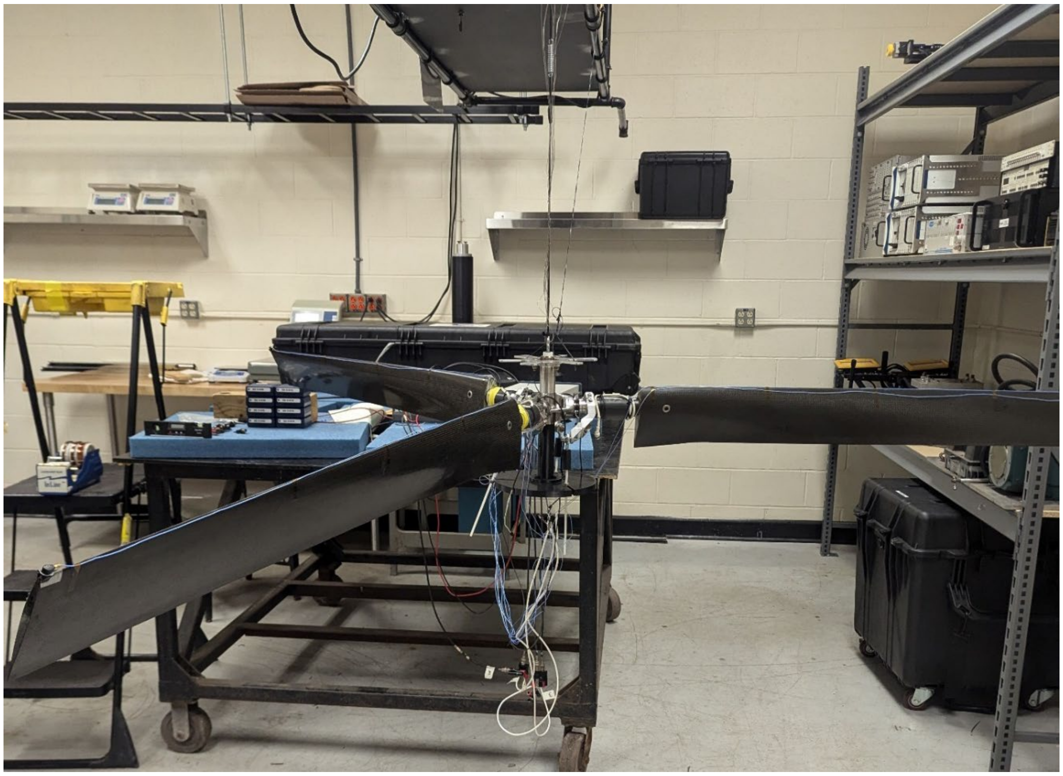

Figure 3. **Hingeless hub (with carbon fiber blades) assembly suspended with inline spring.**

Pitch angles were set by adjusting the throw length of the nylon pitch control rods through the baseplate. On the gimballed hub the installed string potentiometers for blade pitch angle were read using a multimeter and compared directly with pre-tabulated calibration data, while the hingeless hub's potentiometers were calibrated using an inclinometer prior to the test. Due to an error in which the wrong blade twist was used as the offset for the inclinometer, the pitch angles for the hingeless hub tested were all 7.3° higher than initially intended. For testing purposes, all blade pitches were adjusted to be identical, simulating collective control only. As an important note, the gimballed hub introduced some flexibility into the system such that adjusting the pitch of one blade induced gimbal motion, impacting the pitch of the other two blades. As such, an iterative approach was necessary to achieve the desired pitch angles. Additional pictures of the setup can be found in the Appendix (Figures A-1 through A-3).

The GVT itself was conducted using an impact hammer to excite each blade's chord and flap modes, as well as the vertical excitation of the central hub. Each excitation was completed 10 times for every pitch angle chosen to provide a good dataset for analysis. The vibration data itself was collected via single axis accelerometers installed in the chordwise and flapwise directions at the tip of each blade (Figure 4) and a single tri-axis accelerometer located on the hub as near to the center as possible. The data collection and analysis were handled using a Brüel & Kjær (B&K) data acquisition system along with the B&K analysis software.

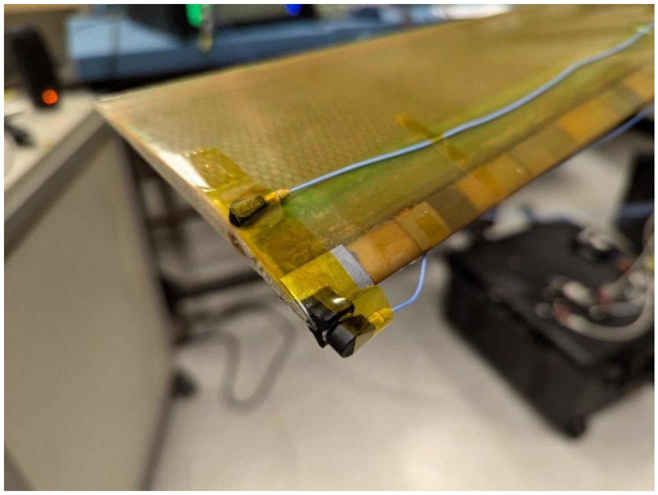

Figure 4. Accelerometers installed on the fiberglass blades (gimballed hub configuration).

3. Analytical Modeling

Analytical modeling for both hubs was conducted using RCAS and NASA Structural Analysis (NASTRAN), while CAMRAD II was only used for the hingeless hub. In each analysis code, the hubs were modeled using free-free boundary conditions with one exception. The vertical translational degree of freedom was modeled with a spring stiffness of 22.66 lbf/inch to match the suspension spring from the experiment.

The linear stability analysis was conducted across a range of collective inputs in each analysis software. Due to slight differences in how collective inputs translate to blade pitch in each program, the collective inputs themselves are not reported. Instead, the corresponding blade pitches are presented in Table 1.

Table 1. Mean absolute and percentage offsets between RCAS analysis and experimental data.

	Gimballed hub w/ fiberglass blades		Hingeless hub w/ carbon fiber blades	
	Δ Hz	**Δ %**	**Δ Hz**	**Δ %**
Symmetric chord	3.42	6.94	1.85	2.27
Asymmetric chord	1.42	6.66	0.66	2.23
Symmetric flap	1.30	7.58	0.32	1.06
Asymmetric flap	2.34	5.54	3.14	5.18

4. Results

In the measured data there is a single symmetric mode and two asymmetric modes for a three-bladed hub. This represents a collective movement of all the blades together and movement of the blade mode about a rotation. While these modeshapes occur at the same frequency in theory, minute differences between the blades cause the responses to have a small frequency offset from one another. To avoid confusing them with higher harmonics, which are not examined in this work, they will be differentiated as asymmetric flap or chord modes A and B. This distinction is not necessary for the analytical models because the blades are modeled as identical and only one frequency presents for each asymmetric mode. Most of the asymmetric modes were readily apparent in experimental testing; however, asymmetric flap mode B could not be identified for the gimballed hub/fiberglass blades due to the tendency of this configuration to generate more frequency noise in the higher ranges during testing.

Figure 5 presents the measured and analytically predicted frequencies of the fiberglass blades with the gimballed hub versus collective pitch. Most of the GVT measurements match the predicted trends, with the analysis codes tending to slightly overestimate the frequency response. The exception is an outlier with respect to the symmetric chord mode at 50° pitch, possibly caused by the interaction between the symmetric chord and asymmetric flap modes as they cross frequencies in that pitch range.

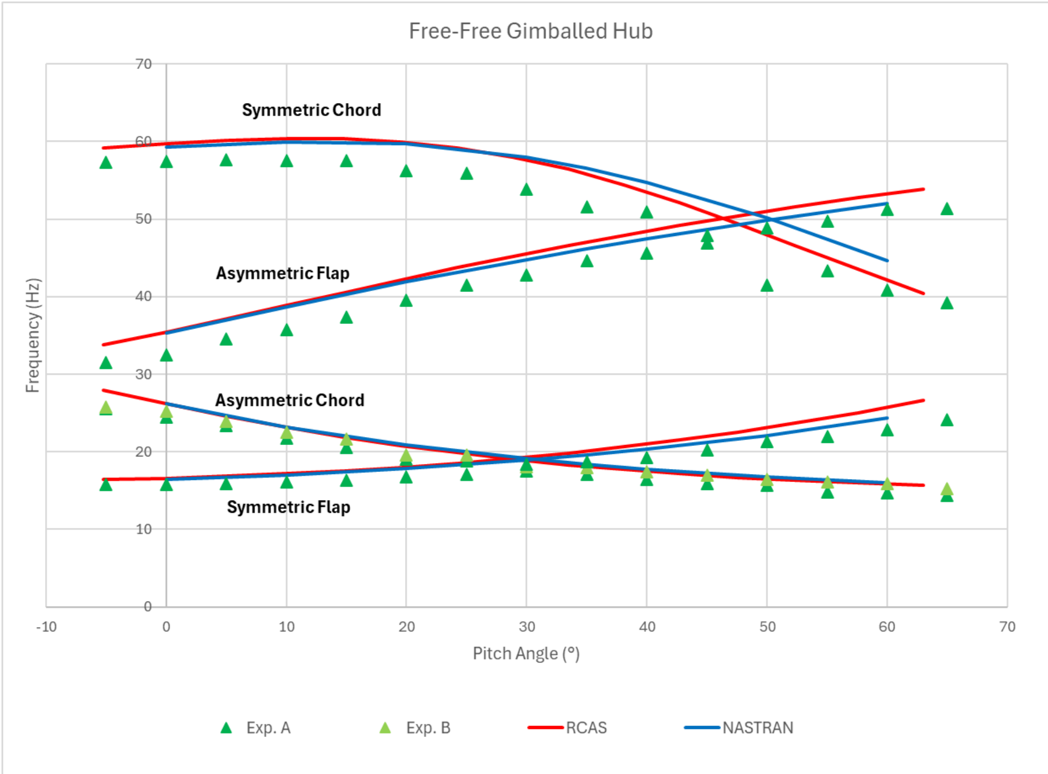

Figure 5. Results of the free-free testing on the gimballed rotor hub (fiberglass blades).

The hingeless hub with the carbon fiber blades (Figure 6) also demonstrated smooth progression. The higher frequency values for all four of the examined modes in this configuration were expected in this analysis. The carbon fiber blades used on the hingeless hub are significantly stiffer than the fiberglass blades installed on the gimballed hub and see a marked increase in frequency response.

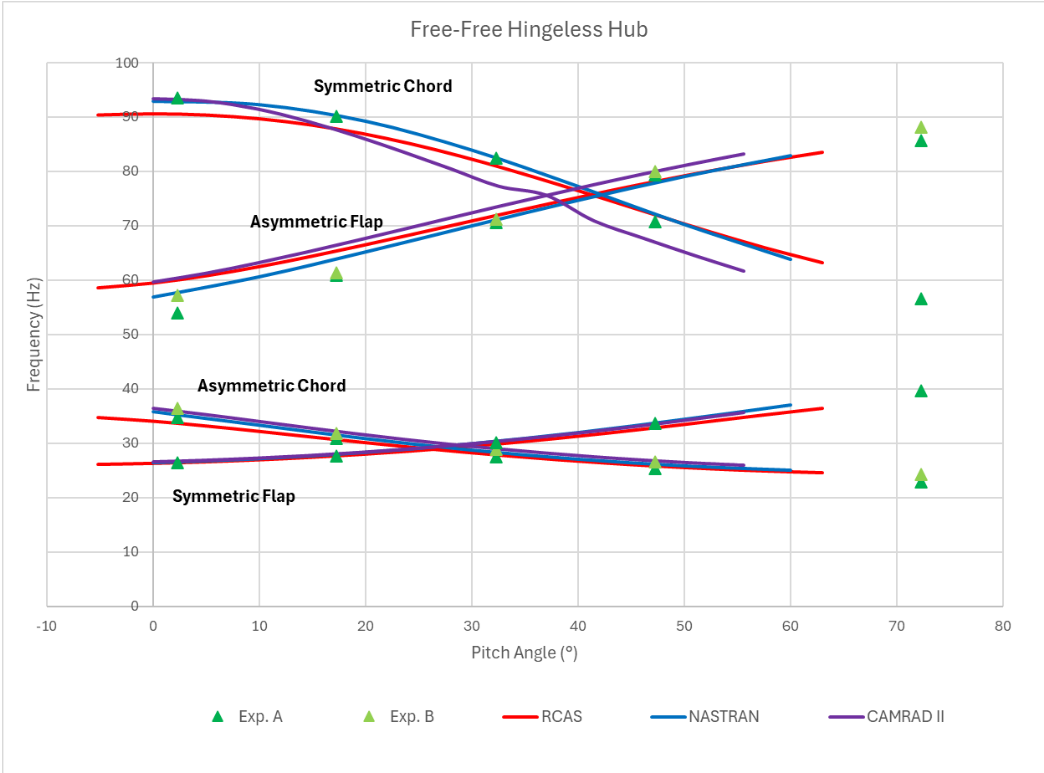

Figure 6. Results of the free-free testing on the hingeless hub (carbon fiber blades).

When plotted against the experimental data, the analytical results showed reasonably good agreement overall. For the gimballed hub/fiberglass blade configuration (Figure 5), the trends are nearly identical for three of the modes despite all theoretical frequency values being higher than experimental values throughout the collective range. The fourth mode (symmetric chord) still provided a reasonable approximation of the modal frequency in the testbed; however, the curve generated in RCAS is notably more convex and has the greatest offset from the experimental results. For the hingeless hub/carbon fiber blade configuration, there is very good agreement between all the analysis software and experimental results in both the symmetric flap and asymmetric chord modes, though there is some overestimation of the latter in the lower collective range. While the general trends are also reasonably predicted for the symmetric chord and asymmetric flap modes, there appears to be some nonlinearity in the responses that are not fully captured in any of the analyses.

To provide a quantitative comparison of the results, it was necessary to generate regression curves for the experimental data. A third-order polynomial regression was used for both hub/blade configurations because inflection points were noted in the experimental data, between 30° to 40° pitch, in the symmetric chord and asymmetric flap modes (Figure 7). The mean absolute offset values for both the gimballed and hingeless hubs (Table 1) were calculated by computing the absolute difference between the RCAS results and the regression curve at each collective angle. The asymmetric B modes were not used for this comparison for the sake of clarity. Additionally, this comparison was conducted only with the RCAS analyses as they covered a wide, relatively even collective range. While these means alone do not speak to the general trend of the frequencies, they do provide a reasonable metric for a rough evaluation of the efficacy of the analysis software. Due to their close agreement with RCAS, it can be assumed that similar results would be apparent for both NASTRAN and CAMRAD II if the analyses were conducted over the same range of values.

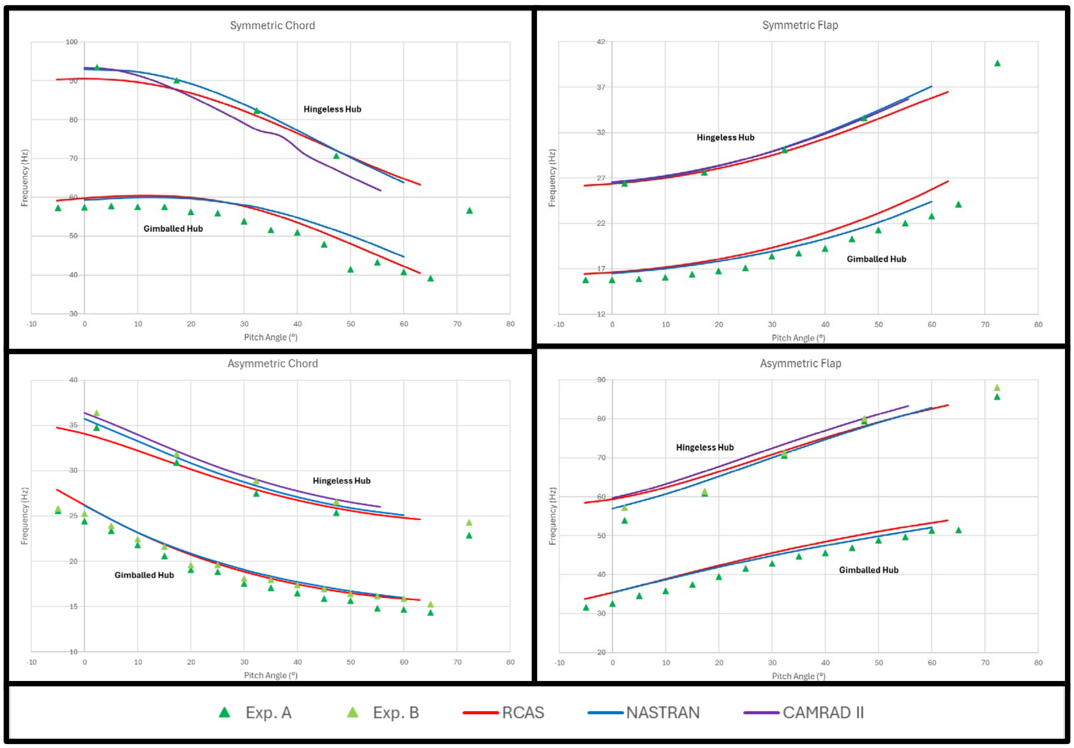

Figure 7. Comparison of the rotor modes for the gimballed hub with fiberglass blades and hingeless hub with carbon fiber blades.

Examining the results for the gimballed hub with the fiberglass blades, the consistently lower experimental data values, as compared with the analytically predicted values, may indicate that the stiffness of the fiberglass blades and/or of the gimballed hub are lower than the estimated values used in the software. For the hingeless hub with the carbon fiber blades, the overall agreement in most of the modes was significantly improved over the gimballed configuration, with the exception of the asymmetric flap mode. The asymmetric flap mode in the hingeless configuration shows more significant trend disagreement in the very low and very high collective ranges. This is likely due to a nonlinearity that is not completely captured in any of the analyses. A similar nonlinearity is visible in the symmetric chord mode; however, it is less pronounced in the tested range.

Of additional note is the behavior of the modeshapes themselves as the blade pitch increased. The chord and flap modeshapes, symmetric and asymmetric, are all defined from the perspective of the rotor hub, with chordwise motion being in-plane with respect to the rotor disk and flapwise being perfectly out-of-plane. At 0° pitch, the chord modeshapes (Figure 8) were characterized by almost perfectly in-plane motion. For the symmetric mode, all three blades lead and lag in a synchronous motion. For the asymmetric modes, a pair of the blades would move opposite one another, making a scissoring motion. The third blade in this situation would lead and lag in sync with one of the other two blades; however, the amplitude of the oscillations was sometimes markedly reduced as compared with the other two blades. The flap modeshapes at 0° (Figure 8) were also isolated to primarily out-of-plane motion. For the symmetric flap, all three blades would rise and fall in sync with one another, while the asymmetric flap mode had each blade approximately 120° out of phase with the preceding blade.

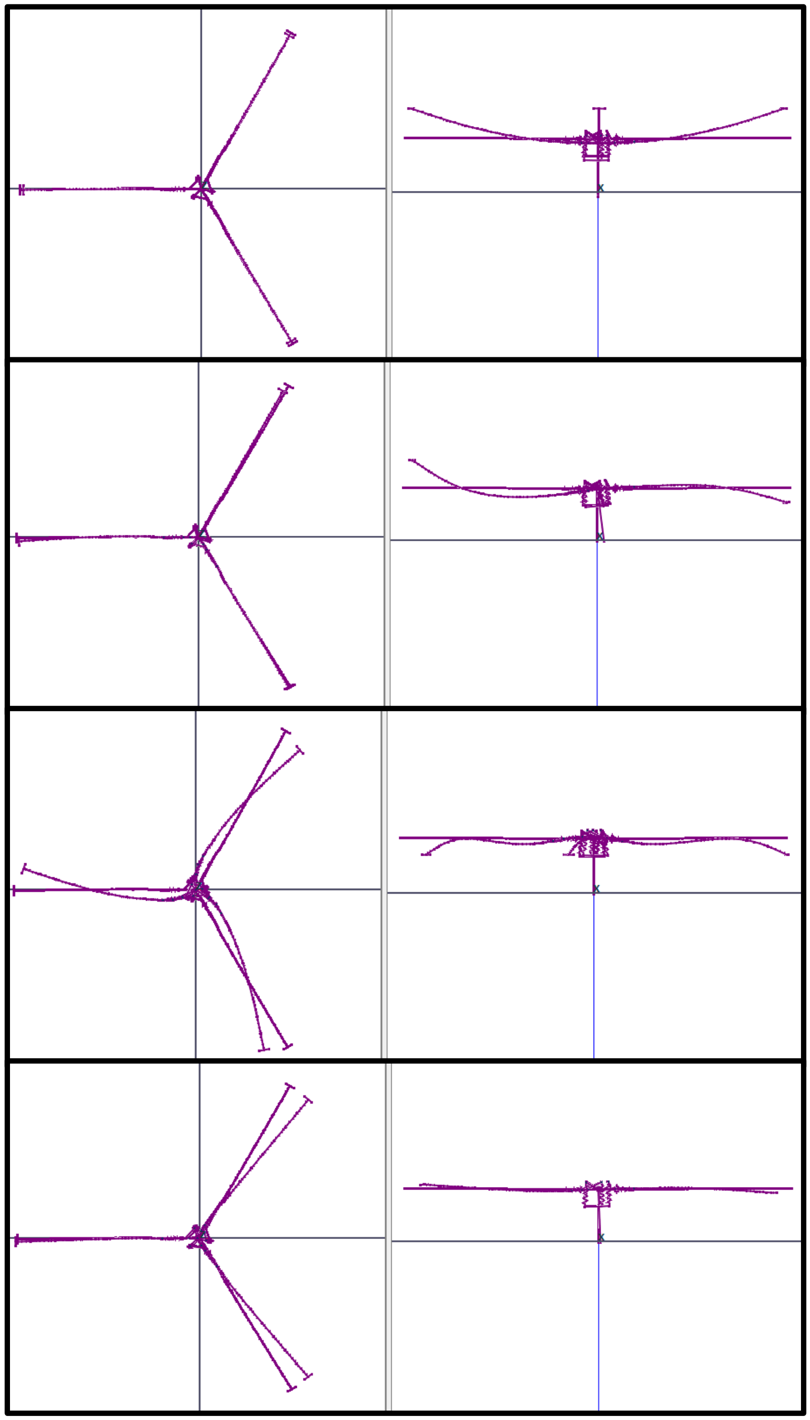

Figure 8. Hingeless hub with carbon fiber blades, 0° pitch top view (left) and front view (right). From top down: symmetric flap, asymmetric flap, symmetric chord, and asymmetric chord.

At high pitch ranges, such as 65° (Figure 9), the behavior of the various modeshapes varied significantly from the lower pitch configurations. The asymmetric chord mode (Figure 9) displayed the least variation, with motion remaining primarily isolated to within the rotor plane. From the perspective of the blade this means that the asymmetric chord mode actually consists of more blade flapping than chordwise motion, as the pitch of the blades orients the chordline (at 3/4 span) mostly out-of-plane. The symmetric flap mode (Figure 9) demonstrates the second least deviation from low pitch configurations. The motion is confined primarily to out-of-plane, though there is a notable in-plane component. Again, though the rotor disk itself is flapping symmetrically, this demonstrates significant chordwise motion of the individual blades in this modeshape. The symmetric chord (Figure 9) mode is mostly in-plane at this range and consists almost entirely of flapwise motion from the perspective of the blades themselves. Little chordwise motion exists along the airfoil. Finally, the asymmetric flap mode (Figure 9) of the rotor exhibits significant deviation from the lower pitch ranges. This modeshape no longer consists of primarily out-of-plane motion and instead appears to be governed almost entirely by the flapwise direction of the individual rotor blades. As such, a significant leading and lagging motion is coupled with the asymmetric disc flapping in these modeshapes, resulting in complex rotor motion.

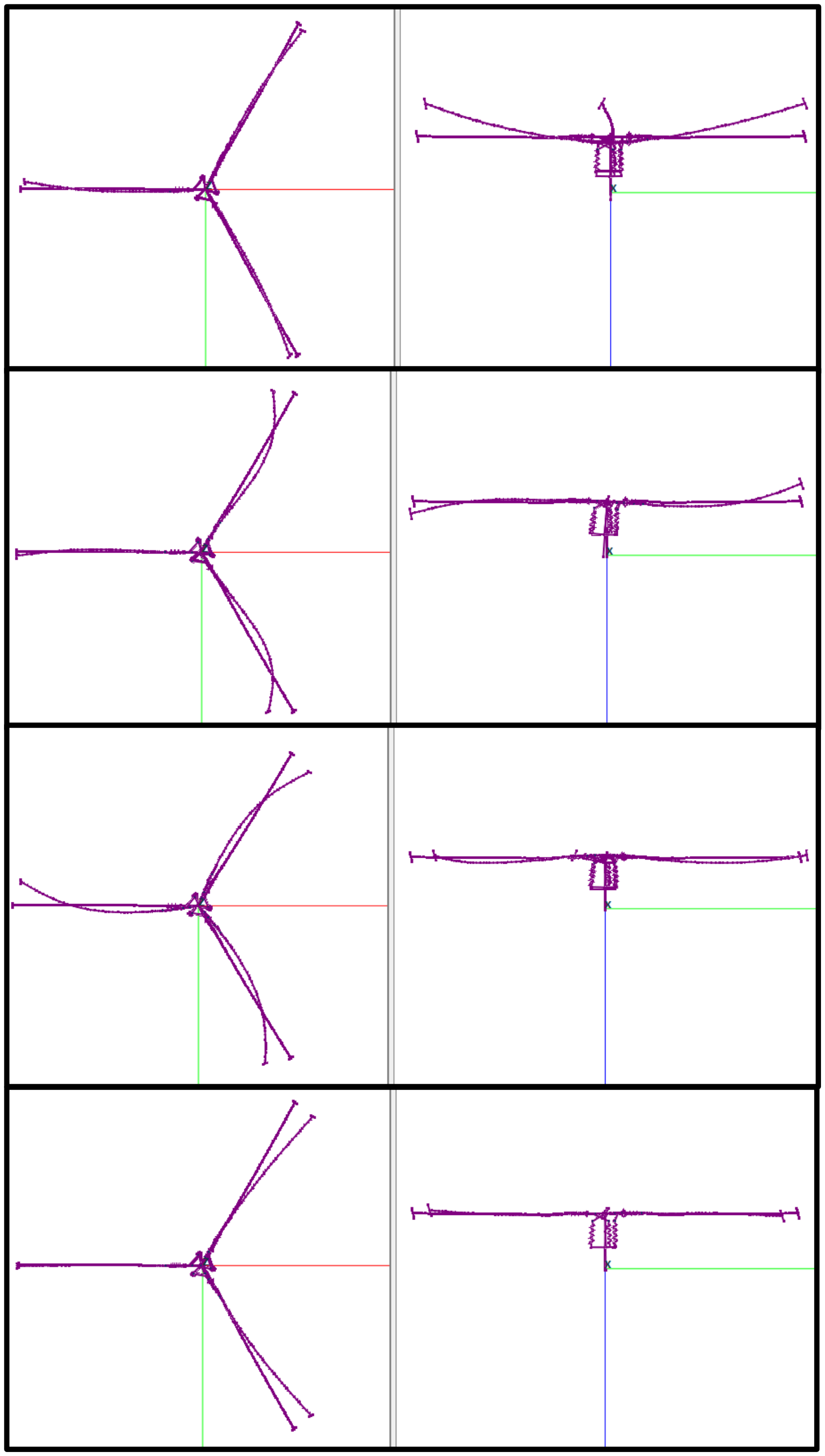

Figure 9. Hingeless hub with carbon fiber blades, 65° pitch top view (left) and front view (right). From top down: symmetric flap, asymmetric flap, symmetric chord, and asymmetric chord.

Because the isolation of these modeshapes to in-plane and out-of-plane motion begins to break down at higher pitch ranges, it is likely that the coupling relationship between these modes and any pylon, wing, or fuselage modes will also evolve with pitch changes. The asymmetric flap mode in particular, being neither in-plane nor perfectly out-of-plane, may be subject to excitation by any forced translation or rotation of the rotor hub.

5. Conclusions

The purpose of this GVT was to generate comparative data between the experimental and analytical models to demonstrate the efficacy of the analytical models in correctly predicting the behavior of the two hub types. For the gimballed hub, the frequency trends of the model were well represented by both RCAS and NASTRAN; however, the frequency offset indicates that both models are likely underestimating the stiffness within the gimballed hub and/or fiberglass blades. For the hingeless hub, the frequencies themselves were better predicted, especially for the symmetric flap and asymmetric chord modes, but the trends of the asymmetric flap and symmetric chord modes both demonstrate some small nonlinearity that is not fully captured in RCAS, NASTRAN, or CAMRAD II. These results indicate that all three analysis systems sufficiently model the rotor mode frequencies throughout the operational collective range; however, the models may benefit from some additional refinement.

Appendix. Additional Experimental Setup Photos

Figures A-1 through A-3 show additional experimental setup images for the gimballed hub as well as an image of the test equipment used in the experiment.

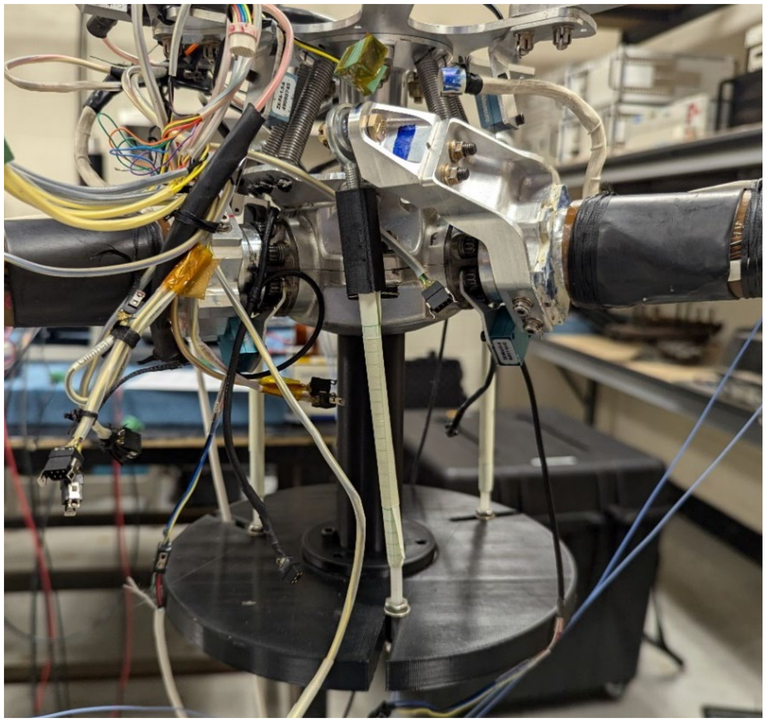

Figure A-1. Gimballed hub installed on 3-D printed baseplate with nylon pitch control rods.

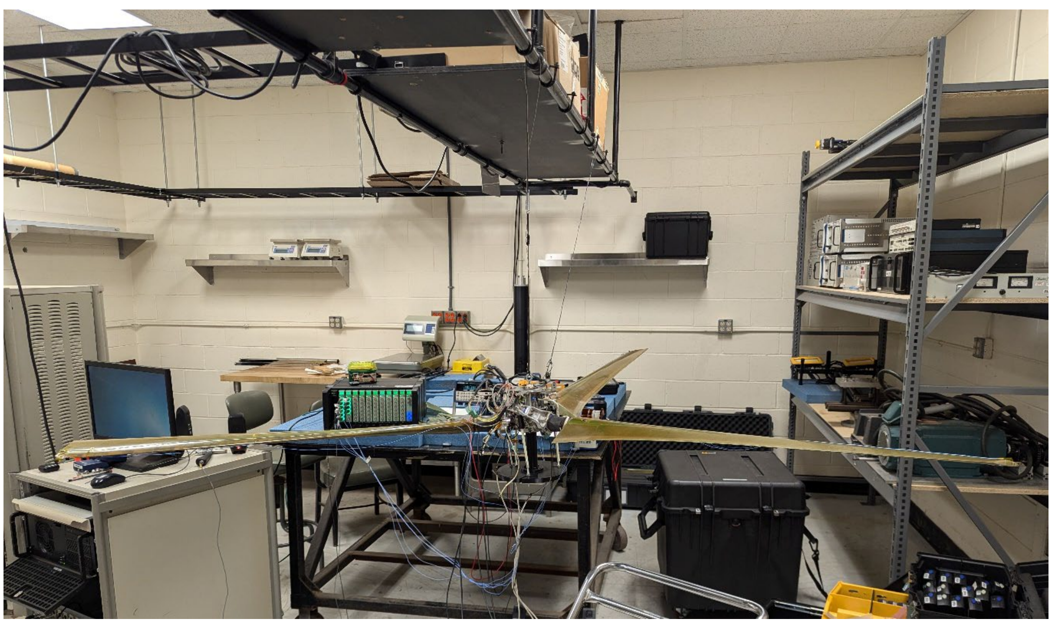

Figure A-2. Gimballed hub assembly suspended with inline spring.

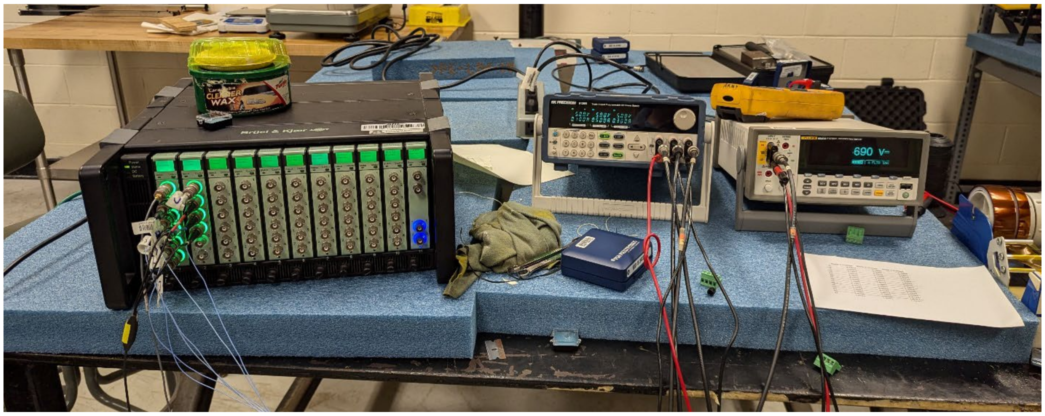

Figure A-3. Test equipment setup with Brüel & Kjær data acquisition system (left), power supply (center), and multimeter (right).

List of Symbols, Abbreviations, and Acronyms

3-D	Three-Dimensional
B&K	Brüel & Kjær
CAMRAD II	Comprehensive Analytical Model of Rotorcraft Aerodynamics and Dynamics
GVT	Ground Vibration Testing
NASA	National Aeronautics and Space Administration
NASTRAN	NASA Structural Analysis
RCAS	Rotorcraft Comprehensive Analysis System
TRAST	TiltRotor Aeroelastic Stability Testbed

1 (PDF)	DEFENSE TECHNICAL INFORMATION CTR DTIC OCA
1 (PDF)	DEVCOM ARL FCDD RLB CB TECH LIB